Caractériser les environnements sonores sur terre

Pierre AUMOND

Université Gustave Eiffel, CEREMA, UMRAE

Workshop SERENADE - 2022

Introduction

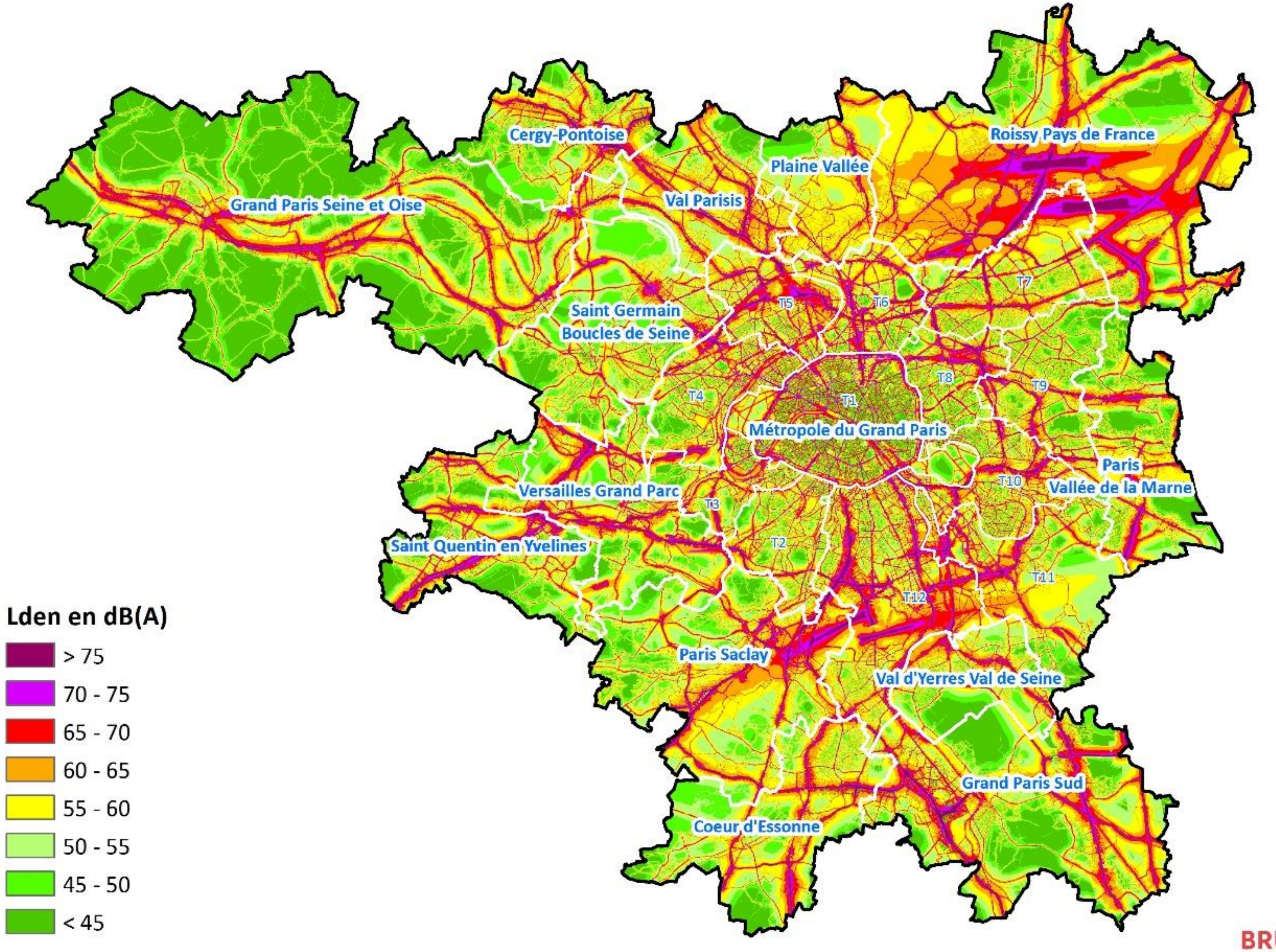
Cergy-Pontoise
Roissy Pays de France
Plaine Vallée
Val Parisis
Grand Paris Seine et Oise
T7
T5
T6
Saint Germain
Boucles de Seine
T8
T9
T4
T1
Métropole du Grand Paris
Paris
Vallée de la Marne
T10
Versailles Grand Parc
T3
Saint Quentin en Yvelines
T2
T11
T12
Lden en dB(A)
> 75
70 - 75
65 - 70
60 - 65
55 - 60
50 - 55
45 - 50
< 45
Paris Saclay
Val d'Yerres Val de Seine
Grand Paris Sud
Coeur d'Essonne
BRUITPARIF

Caractériser les environnements sonores

- Directive 2002/EC/49
- Modèle harmonisé au niveau européen

Caractériser les environnements sonores

- Précision ?
- Les outils ?
- La perception ?
- Utiliser des mesures ?

I. Des modèles

Cartographier et prédire les environnements sonores

Standardisé

“Standard” noise models

- **CNOSSOS–like / Geometrical approaches**

Emission model
Road trafic
Rail trafic
Air trafic

Path-finding algorithm

Attenuation model

Salomons, E., Van Maercke, D., Defrance, J., & de Roo, F. (2011). The Harmonoise sound propagation model. *Acta acustica united with acustica*, *97*(1), 62-74.

Kephalopoulos, S., Paviotti, M., & Anfosso-Lédée, F. (2012). Common noise assessment methods in Europe (CNOSSOS-EU). Common noise assessment methods in Europe (CNOSSOS-EU), 180-p.

“Standard” noise models

Geometry & sound power of the sources

Source characteristics as :

- Speed
- Contact surface (pavement, rugosity, …)
- Vehicule type (light vehicule, heavy vehicule, fret, …)
- Environmental conditions (temperature)
- Slope, distance to intersection
- etc.

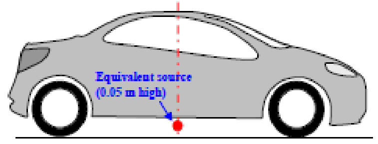

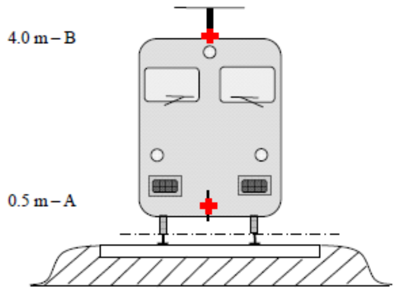

Empiric model

Rolling noise
Propulsion noise
Aerodynamic noise

\+ Flow Rate

$$L_{W',eq,line,i,m} = L_{W,i,m} + 10 \times \lg\left(\frac{Q_m}{1000 \times v_m}\right)$$

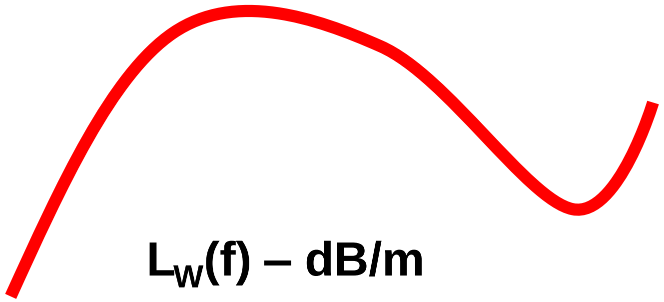

$L_W(f)$ – dB/m

(different heights & directivities)

“Standard” noise models

- Topography
- Geometry & acoustic characteristics of the obstacles
- Geometry & nature of the ground
- Occurrences of meteorological downward-refraction conditions in all the or each propagation direction concerned.
- Others meteorological factors

conditions homogènes

$L_H = L_W + A_H$ avec L_W le niveau de puissance de la source et
$A_H = A_{div} + A_{atm} + A_{sol} + A_{dif} + A_{meteo,H}$

conditions favorables

$L_F = L_W + A_F$ avec L_W le niveau de puissance de la source et
$A_F = A_{div} + A_{atm} + A_{sol} + A_{dif} + A_{meteo,F}$

Outils

NoiseModelling

- from 2010
- initial goal : by and for researchers
- CNOSSOS-EU model
- Java libraries
- GIS databases connection
- Basic user-interface

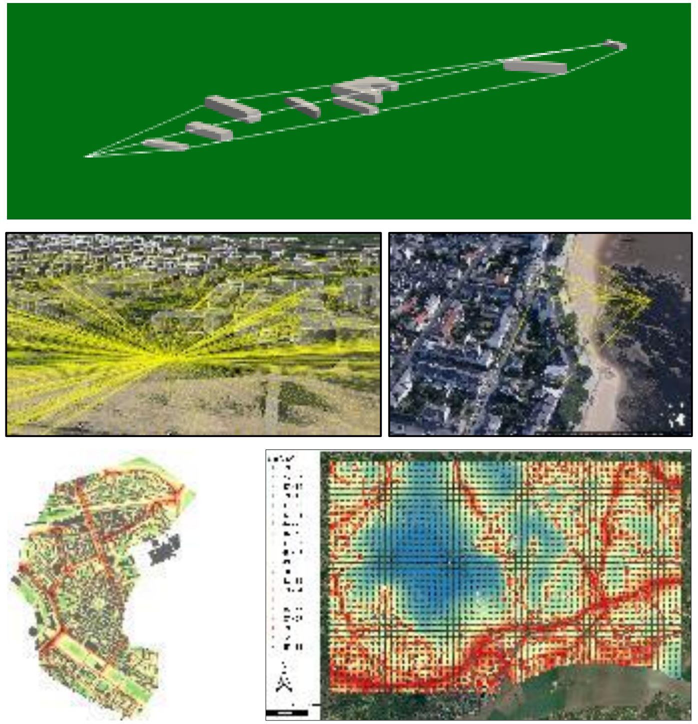

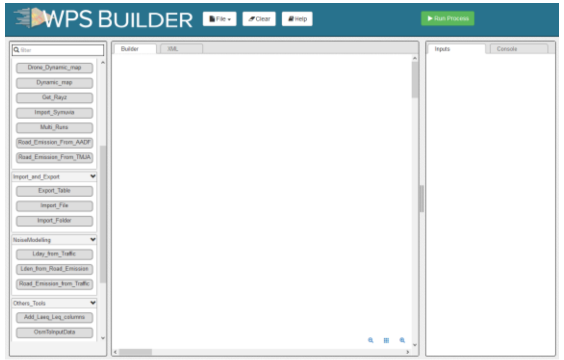

Open-Source

- Open science
- reproducibility
- traceability
- transparency

- NoiseModelling
- Sound Mapping Tools ArcGIS toolbox
- QGIS plugin OpenoiseMap

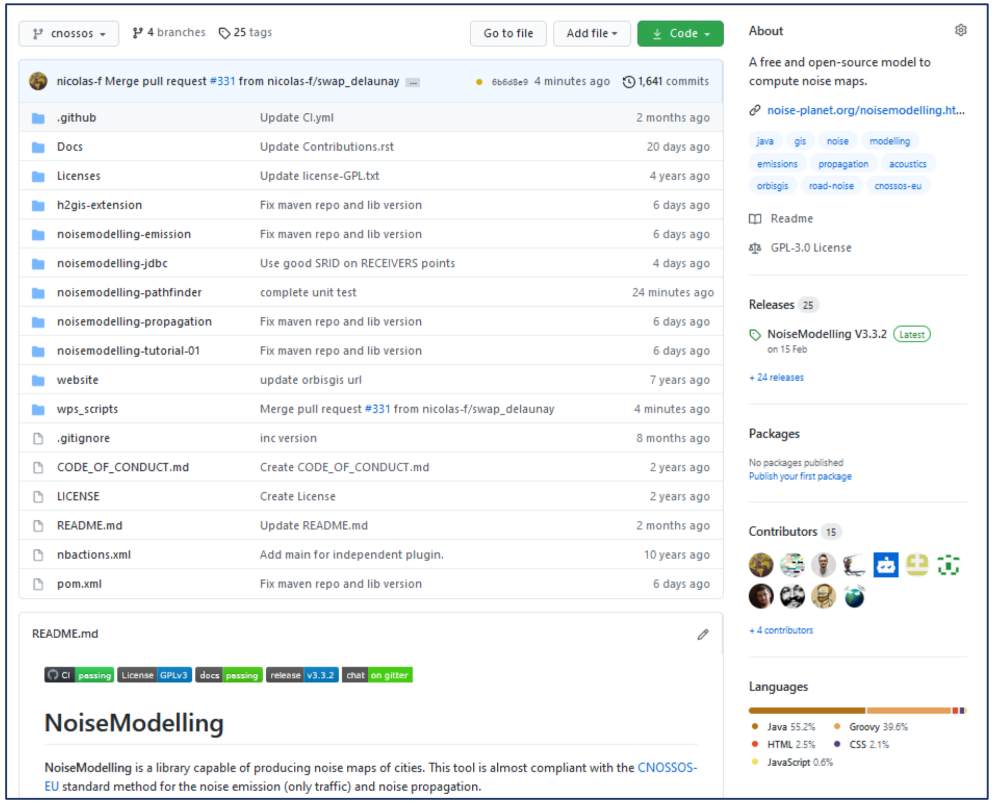

Modèles de référence

Modèles de références

Table 1
Level of appropriateness of computational urban acoustics methods regarding prediction of urban sound at microscale: (–) low, (o) medium or (+) high.

Method	Type[a]	Meteo			Reflection		Diffraction	Frequency	
		Mean profiles	Turbulence	Air Abs.	Geometry	Materials		Storage[b]	Acceleration[c]
PSTD [31,32,111,112]	TD	+	+	+	o[d]	–[e]	+	+	+
FDTD [27,106,113]	TD	+	+	o[f]	o[d]	+	+	o[g]	+
BEM [28,114]	FD	–[h]	–[h]	o[i]	+	o[j]	+	o[g]	o[i]
FM BEM [29]	FD	–[i]	–[i]	o[i]	+	o[j]	+	+	o[i]
ESM [25,26]	FD	–[h]	–[h]	+	o[d]	o[j]	+	o[g]	o[i]
TLM [33,115–117]	TD	+	+	+	o[d]	+	+	o[g]	+
PE [34,35]	FD	+	+	o	–[h]	o[j]	o[k]	o[g]	o[i]
modal/FEM [30]	FD	o[i]	o[i]	o[i]	–[h]	o[j]	+	o[g]	o[i]

[a] Time domain method (TD) or Frequency domain method (FD).
[b] Storage refers to the needed storage capacity of the method.
[c] Acceleration through parallel implementation on CPUs and/or GPUs.
[d] Staircase approximation.
[e] Frequency independent boundary conditions.
[f] Classical attenuation only.
[g] Large number of grid points, see Table 2.
[h] Simplified approaches only.
[i] Although this should be possible, it has not been encountered for urban acoustics applications.
[j] Locally reacting surface impedance.
[k] Kirchhoff approximation.

Table 2
Requirement of number of points per wavelength ppλ for accurate results in urban acoustics (as reported by cited work) and number of discrete points in a 20 m × 20 m × 300 m street, and 2D cross section of sound propagation over an urban area 100 m × 2000 m, up to the 1.6 kHz third octave band. A sound speed of c = 340 m/s has been used.

Method	Volume (V) or Boundary (B) discretization method	ppλ (–)	Number of points	
			3D street	2D urban section
			$\times 10^9$	$\times 10^6$
PSTD [31,32]	V	2	0.14	22.32
FDTD [27] [a]	V	10	17.68	558.03
TLM [33]	V	10	17.68	558.03
BEM [28]	B	6–10	0.02–0.05	0.13–0.21[b]
FM BEM [29]	B	6–10	0.02–0.05	0.13–0.21[b]
ESM [25,26]	B	10	0.05	0.21[b]
PE	V	10	17.68 [35]	558.03[b] [34]
Modal/FEM	B[c]	10	0.03[d]	–[e]

[a] A lower ppλ number is feasible, but has not been presented in urban acoustics applications.
[b] A discretization length of 4000 m is assumed.
[c] 2D intersections are discretized in the 3D model.
[d] 2D intersections every 10 m are assumed.
[e] Model is applied in 3D only.

Ten questions concerning computational urban acoustics – Hornikx, 2016

Equation Parabolique

Fort développement pour le bruit éolien.

Equation Parabolique

Proche de la source ? (EWAPE)

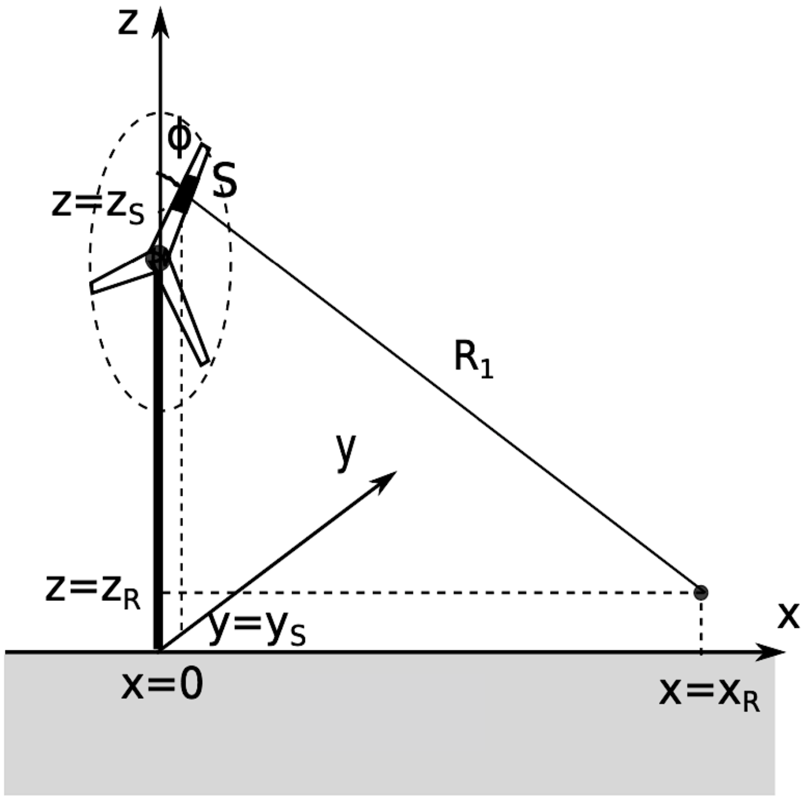

JASA ARTICLE

Wave and extra-wide-angle parabolic equations for sound propagation in a moving atmosphere

Vladimir E. Ostashev,[a)] D. Keith Wilson, and Michael B. Muhlestein[b)]
United States Army Engineer Research and Development Center, 72 Lyme Road, Hanover, New Hampshire 03755, USA

ABSTRACT:
The narrow-angle parabolic equation (NAPE) with the effective sound speed approximation (ESSA) is widely used for sound and infrasound propagation in a moving medium such as the atmosphere. However, it is valid only for angles less than 20° with respect to the nominal propagation direction. In this paper, the wave equation and extra-wide-angle parabolic equation (EWAPE) for high-frequency (short-wavelength) sound waves in a moving medium with arbitrary Mach numbers are derived without the ESSA. For relatively smooth variations in the medium velocity, the EWAPE is valid for propagation angles up to 90°. Using the Padé (n,n) series expansion and narrow-angle approximation, the EWAPE is reduced to the wide-angle parabolic equation (WAPE) and NAPE. Versions of these equations are then formulated for low Mach numbers, which is the case that is usually considered in the literature. The phase errors pertinent to the equations considered are studied. It is shown that the equations for low Mach numbers and the WAPE with the ESSA are applicable only under rather restrictive conditions on the medium velocity. An effective numerical implementation of the WAPE for arbitrary Mach numbers in the Padé (1,1) approximation is developed and applied to sound propagation in the atmosphere. https://doi.org/10.1121/10.0001397

(Received 23 March 2020; revised 21 May 2020; accepted 25 May 2020; published online 17 June 2020)
[Editor: Philippe Blanc-Benon] Pages: 3969–3984

Equation Parabolique

Admittance effective

sol plan + effet moyen de la rugosité sur la diffusion des ondes.

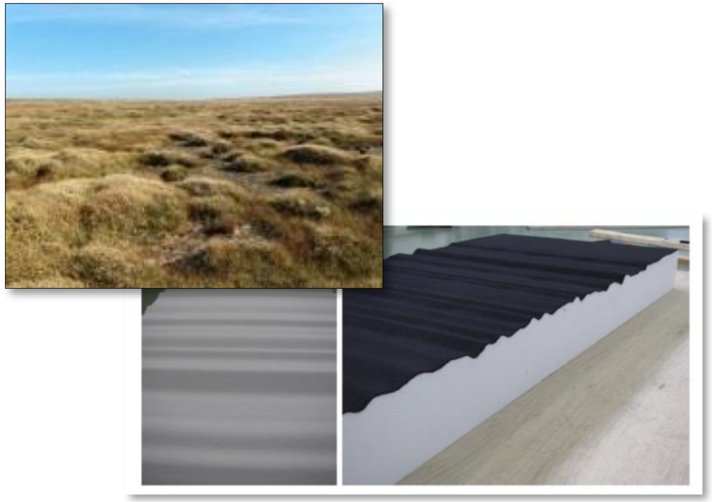

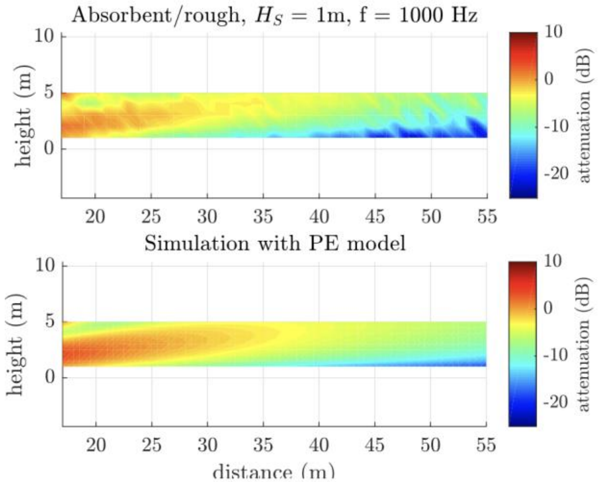

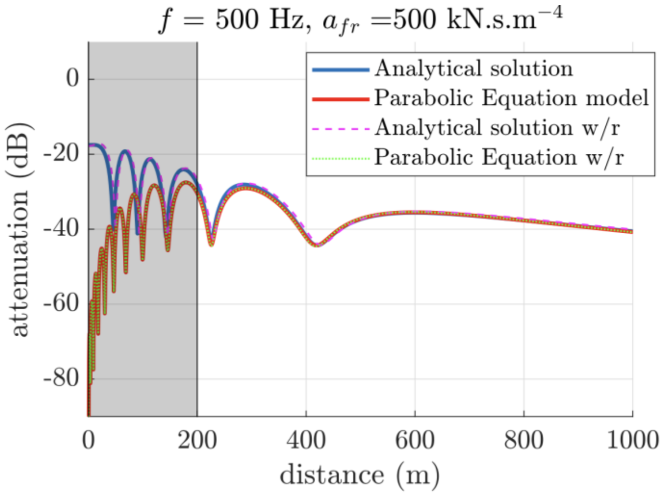

B. Kayser, et. al., Sensitivity analysis of a parabolic equation model to ground impedance and surface roughness for wind turbine noise. *The Journal of the Acoustical Society of America*, 2019

Equation Parabolique

Sol, Relief, Atmosphère

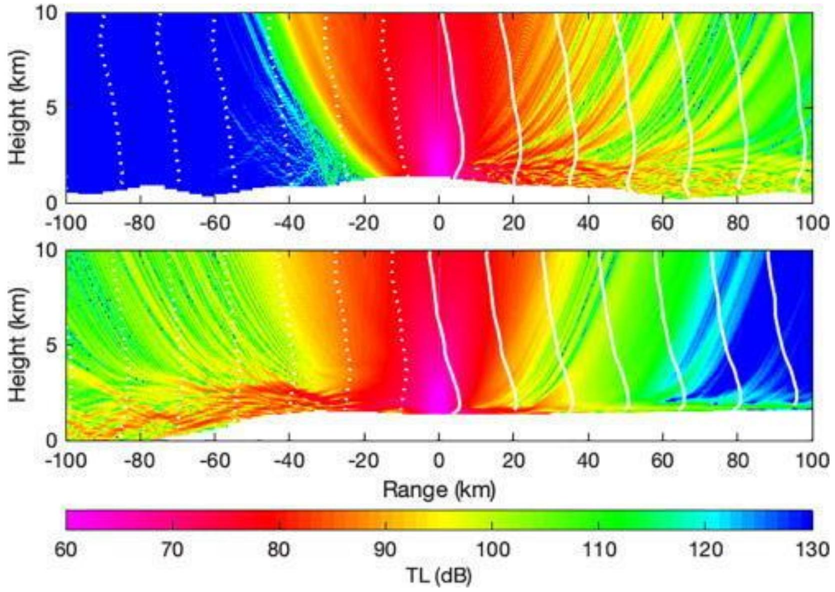

Wilson, D. K., Shaw, M. J., Ostashev, V. E., Muhlestein, M. B., Alter, R. E., Swearingen, M. E., & McComas, S. L. (2022). Numerical modeling of mesoscale infrasound propagation in the Arctic. *The Journal of the Acoustical Society of America*, *151*(1), 138-157.

3D

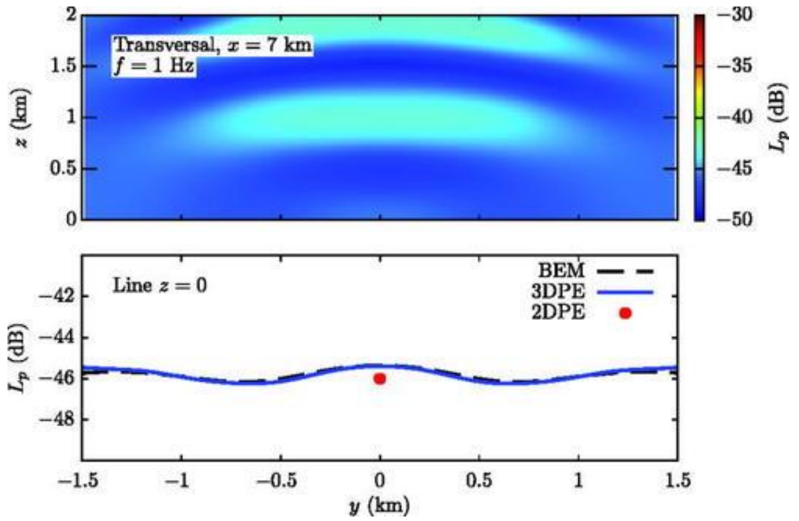

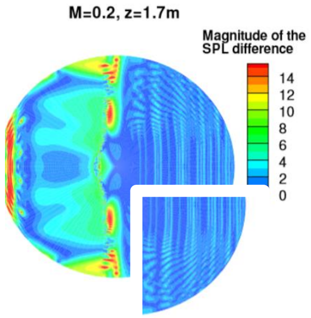

Khodr, C., Azarpeyvand, M., & Green, D. N. (2020). An iterative three-dimensional parabolic equation solver for propagation above irregular boundaries. *The Journal of the Acoustical Society of America*, *148*(2), 1089-1100.

Equation Parabolique

Eolien Offshore ?

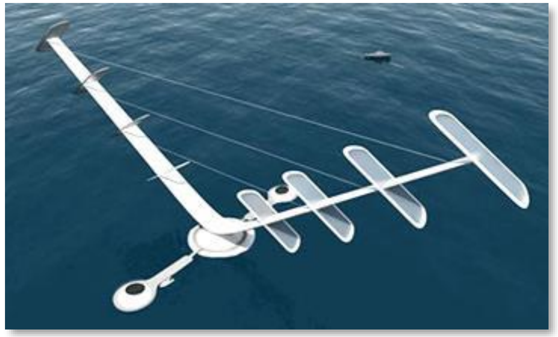

Bill Kayser, Benoit Gauvreau
~~Pierre Aumond, UMRAE~~

Autres modèles de référence

Auralisation

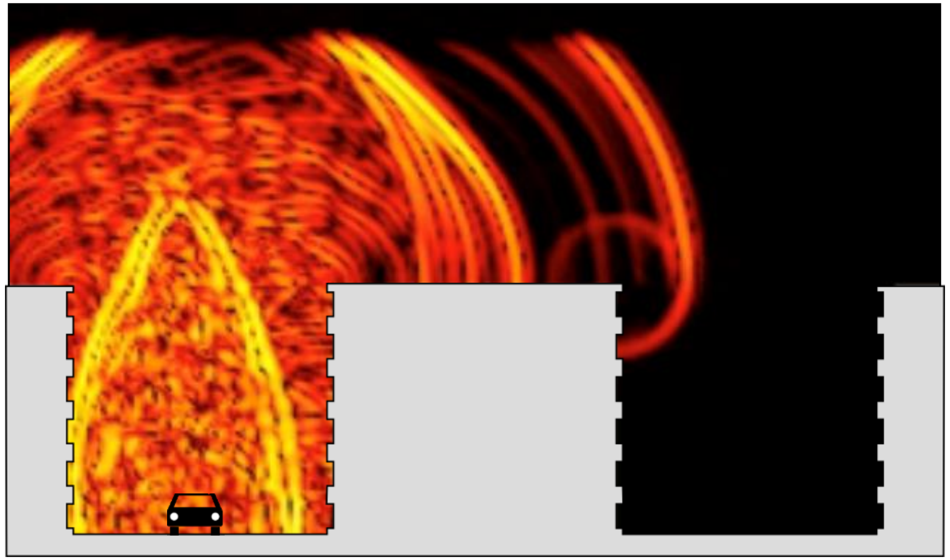

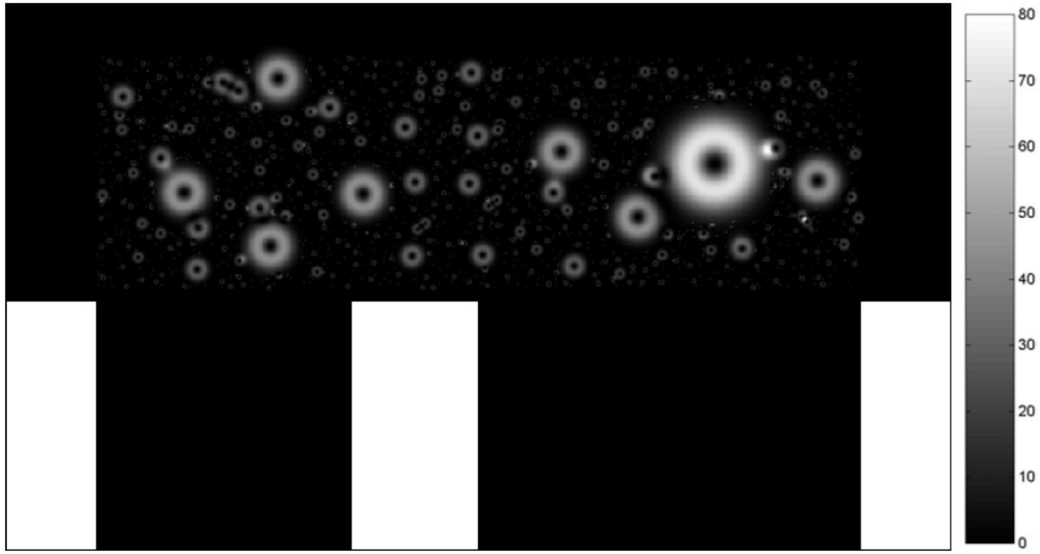

Figure 3.53 Turbulent kinetic energy field $0.5|v_i|^2$ (in m²/s²) for a single realization of the homogeneous, two-dimensional turbulent flow field. The C_v^2 in two dimensions is 10/9 $m^{4/3}/s^2$.

T. Van Renterghem, 2006. Parameter study of sound propagation between city canyons with a coupled FDTD-PE model.
M. Hornikx et al. 2016. openPSTD: The open source pseudospectral time-domain method for acoustic propagation.

Van Renterghem, T., 2004. The finite-difference time-domain method for simulation of sound propagation in a moving medium.

Cartographie à bas-coût

Utilisation de données libres

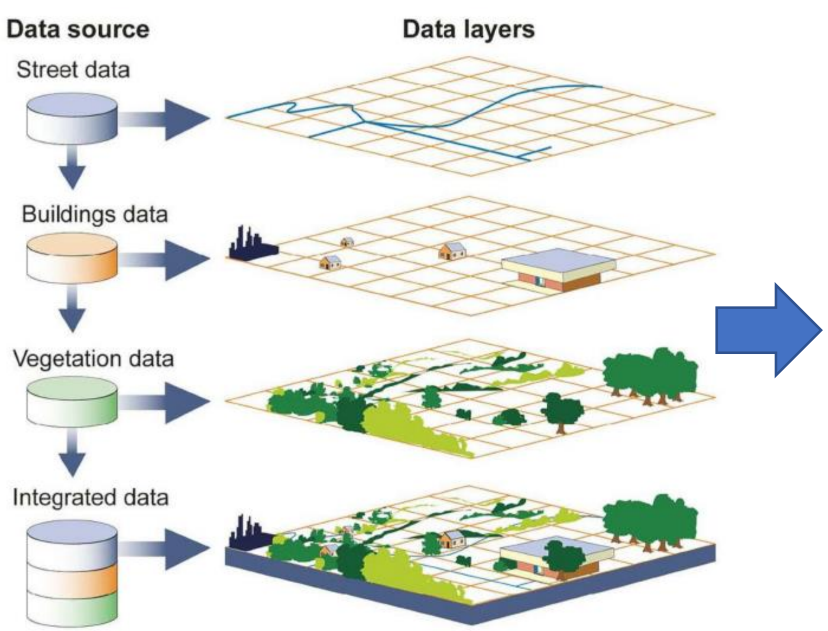

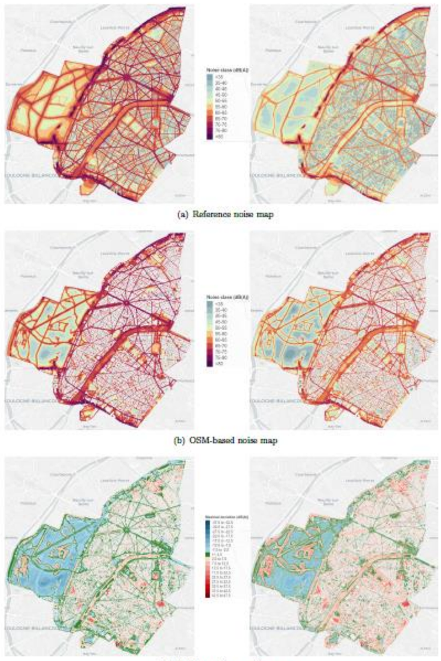

(a) Reference noise map

(b) OSM-based noise map

(c) OSM vs reference noise map

Figure 10. Noise maps for (left) Lden and (right) Ln.

- Presque tous les jeux de données peuvent être trouvé sauf….
- **Les données de traffic routier**

« Noise Mapping based on OpenStreetMap data », E Bocher · 2019
https://github.com/lukasmartinelli/osm-noise-pollution , 2015

Inférence statistique pour modèles bas-coût

Variables	Coefficient
(Intercept)	43.32
Traffic lights	1.28
Crosswalks	0.83
Road surface condition	2.51
Lanes	1.60
Law enforcement authorities	−4.76
Bus routes	1.01
Schools	2.69
Floors in buildings	2.19
Street length	0.006
Bus stops	−0.64
Shops	−0.14

Noise Estimation Using Road and Urban Features, G.R Gozalo et al., 2020

TABLE I. Input variables considered by the network.

1	Time of day
2	Commercial or leisure environment
3	Construction work in the area
4	Stabilization time
5	Traffic flow type
6	Ascendant light vehicle flow
7	Descendant light vehicle flow
8	Ascendant motorcycle flow
9	Descendant motorcycle flow
10	Ascendant heavy vehicle flow
11	Descendant heavy vehicle flow
12	Number of vehicles with siren
13	Abnormal events related to traffic
14	Abnormal events unrelated to traffic
15	Average vehicle speed
16	Road slope
17	Number of ascending lanes
18	Number of descending lanes
19	Pavement type
20	State of the pavement
21	Street type
22	Street width
23	Average building height
24	Road width
25	Distance from noise source

A neural network based model for urban noise prediction, Genaro et al., 2010

Nouvelles méthodologies

Intégration de la dynamique temporelle

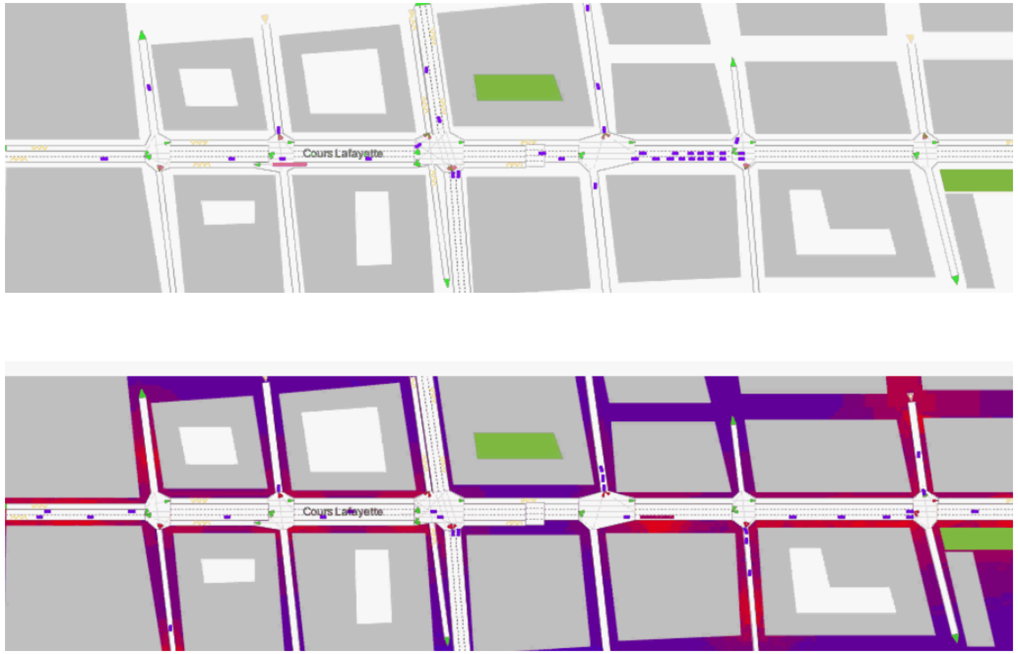

Arnaud Can et al. 2015

Guillermo Quintero et al., 2018

Intégration de la dynamique temporelle

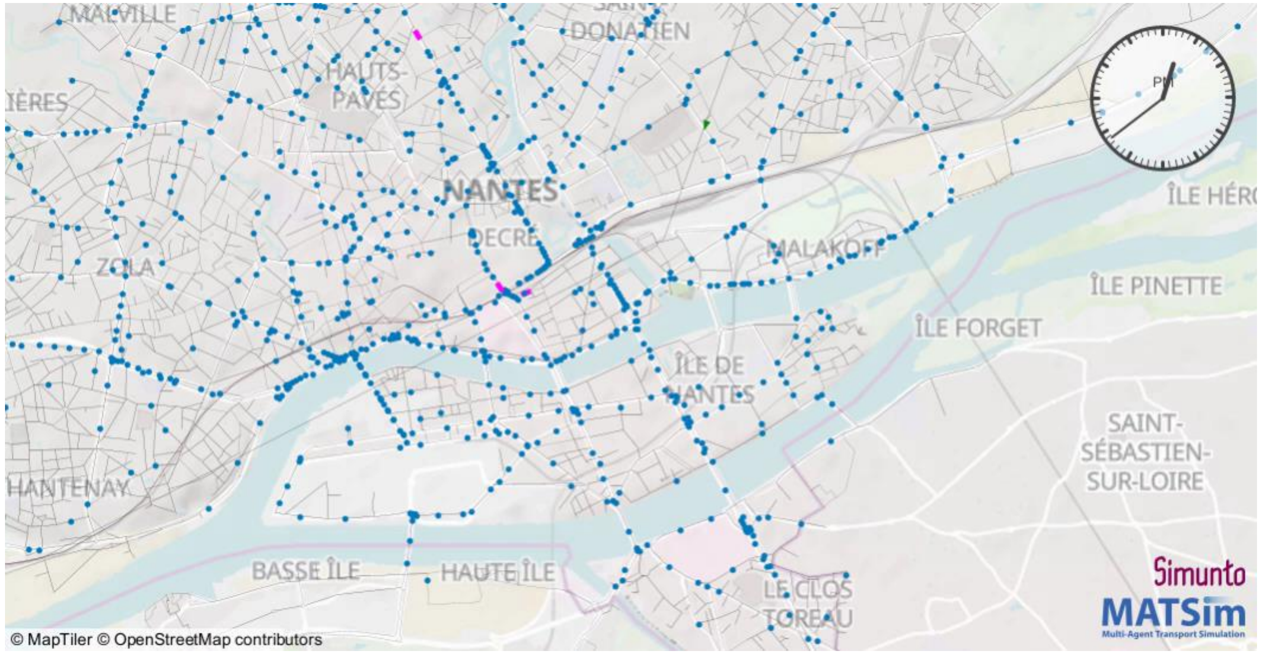

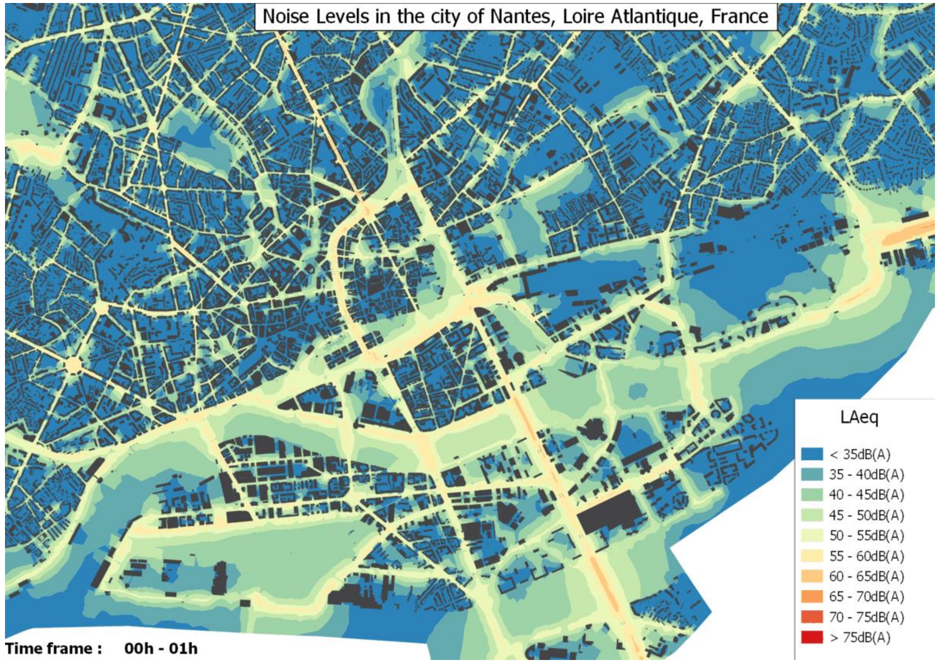

Valentin Lebescond et al. 2018

Intégrer plus de sources sonores

Spatio-temporal activity model

Sound emission model

Voices

Bird songs

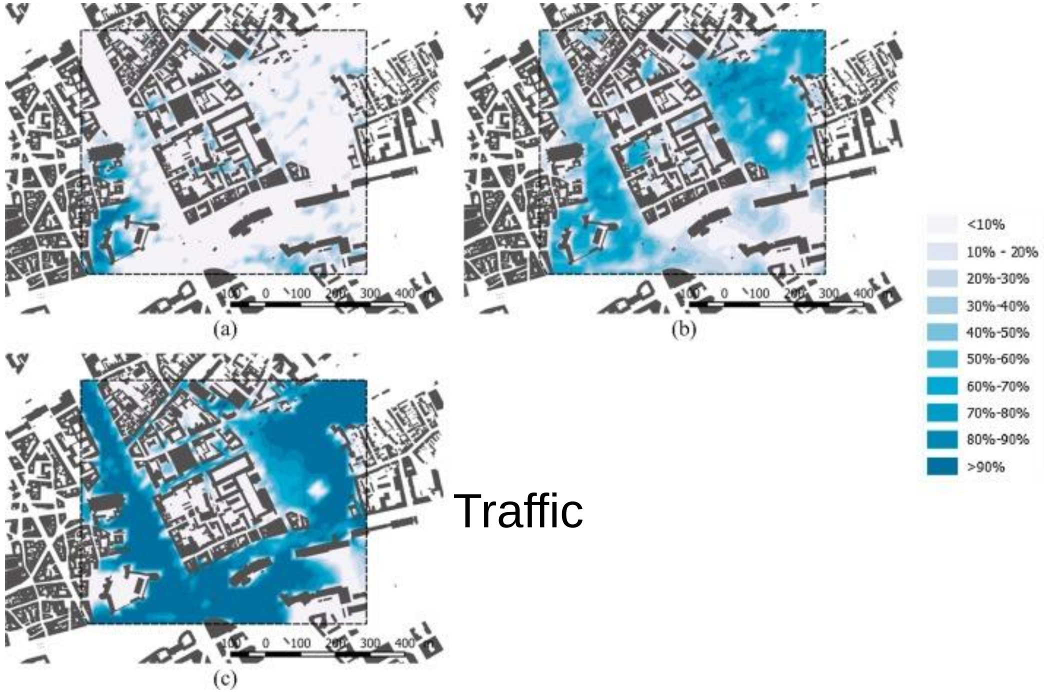

Traffic

Probabilistic modeling framework for multisource sound mapping, Aumond et al. 2018

Meta-Modèles

Meta-model

$$\widehat{\mathcal{M}}(\mathbf{p}) = \hat{w}_1(\mathbf{p}) \times map_1 + \hat{w}_2(\mathbf{p}) \times map_2 + \ldots + \hat{w}_k(\mathbf{p}) \times map_k$$

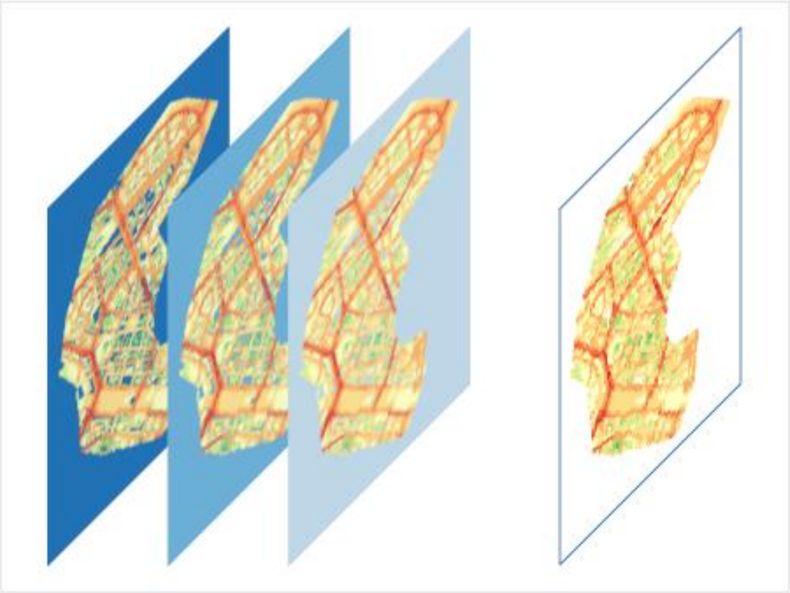

Lesieur, 2019

Meta-Modèles

Lesieur, 2019

Meta-Modèles

Qualitatif

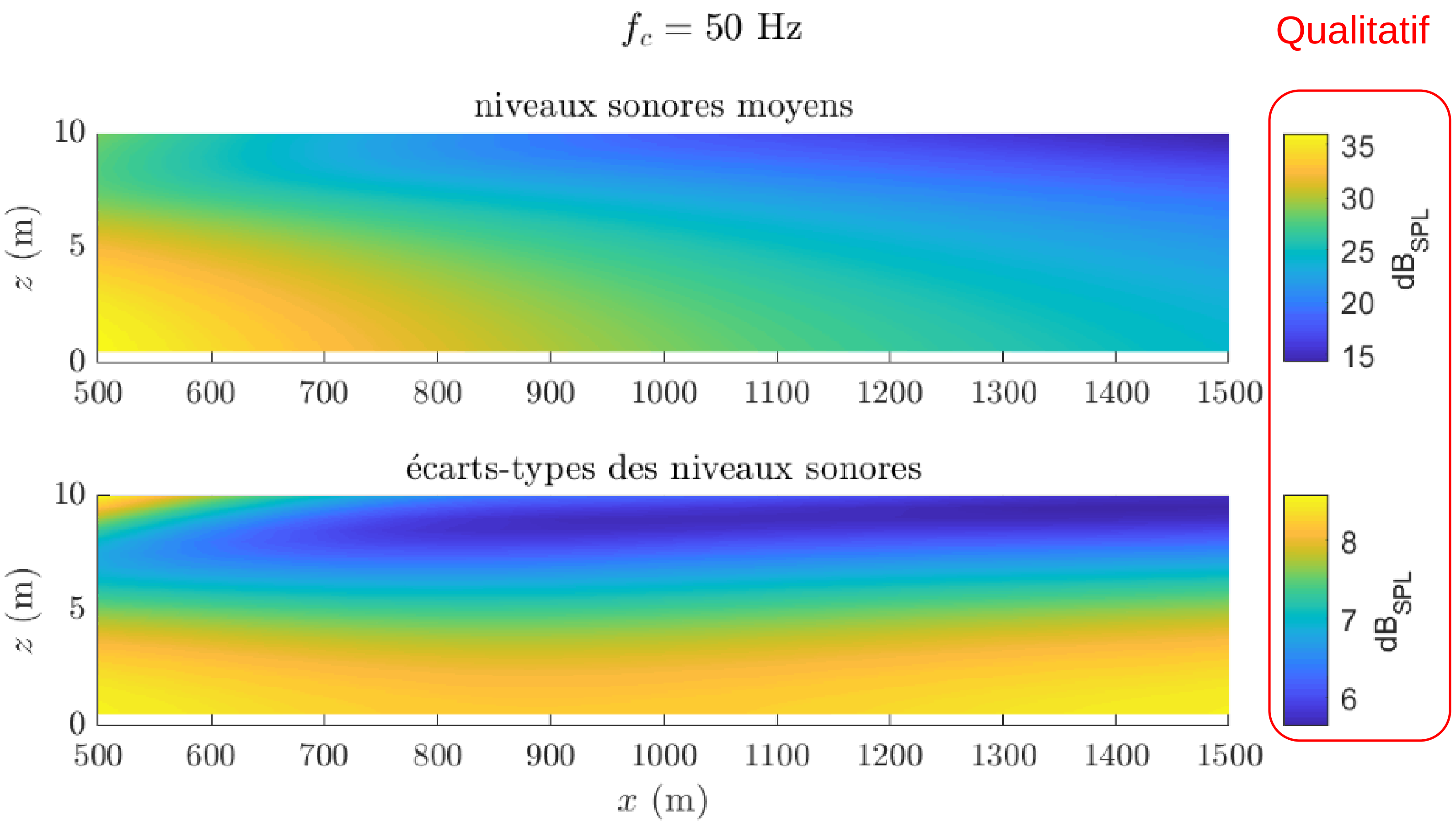

Enjeux en termes de niveaux sonores

Enjeux en termes de variabilité

II. Des observations

Cartographier et prédire les environnements sonores

Réseau de capteurs « Low-cost »

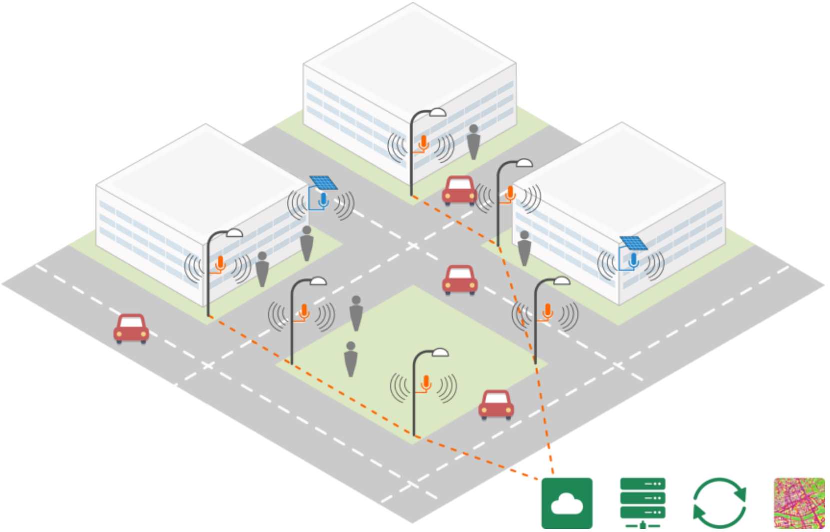

ANR CENSE, Lorient

cense

Ok labs, Germany

„Environmental noise is open data“

J. Picaut et al. 2021 - Low-Cost Sensors for Urban Noise Monitoring Networks—A Literature Review

Mesures mobiles

E. Bocher et al., 2018 Noise mapping based on participative measurements.

Turn your mobile phone into an environmental sensor and participate in the monitoring of noise pollution

Observations + Modèles

Assimilation de données

Bias	RMSE
$\frac{1}{n}\sum_{i=1}^{n}(c_i - o_i)$	$\sqrt{\frac{1}{n}\sum_{i=1}^{n}(c_i - o_i)^2}$

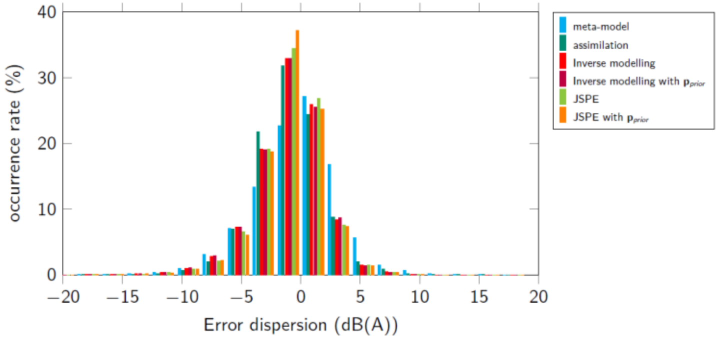

Antoine Lesieur, 2021

III. Le paysage sonore en acoustique environnementale

Le « Paysage Sonore » en acoustique environnementale

“**Acoustic environment** as perceived or experienced and/or understood by a **person or people**, in **context**”

ISO 12913-1:2014

Acoustique — Paysage sonore

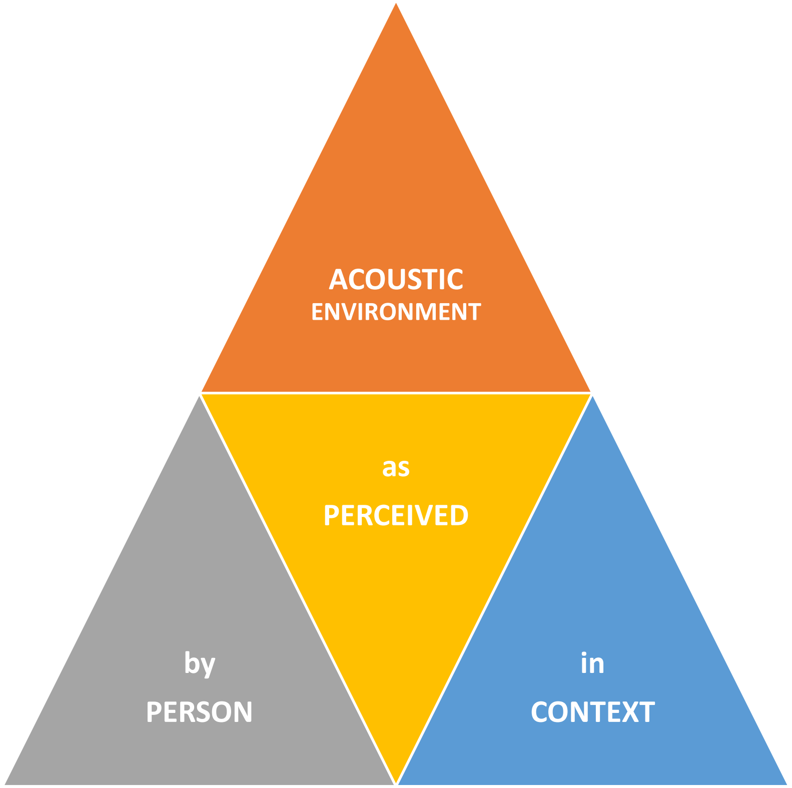

Cartographies du paysage sonore

« Qualité »

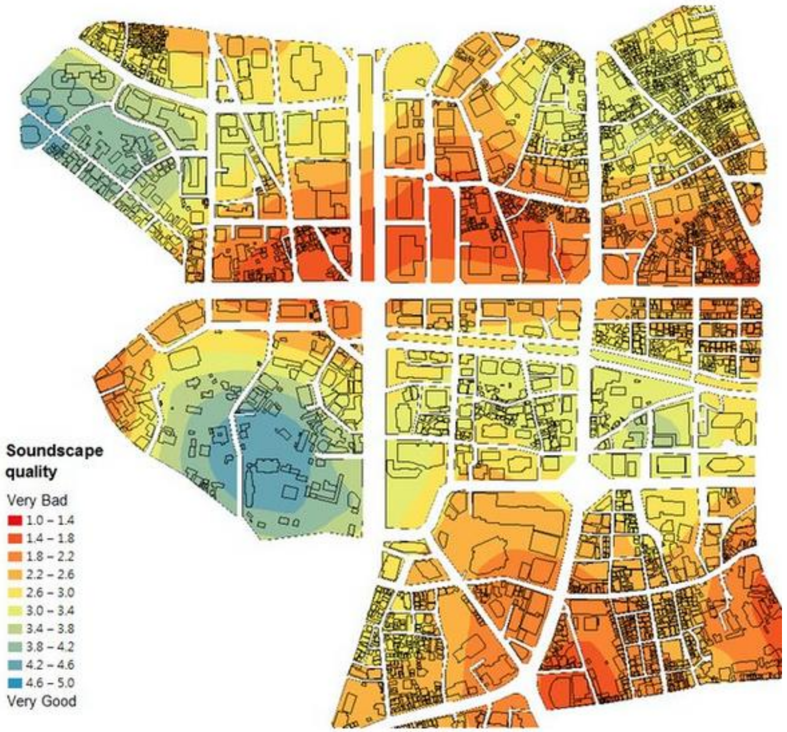

« Approprié »

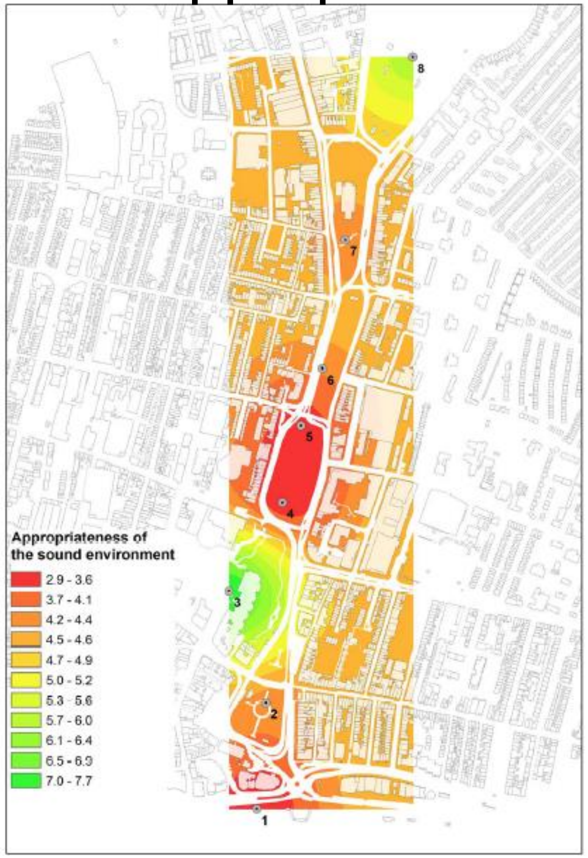

« Agréable »

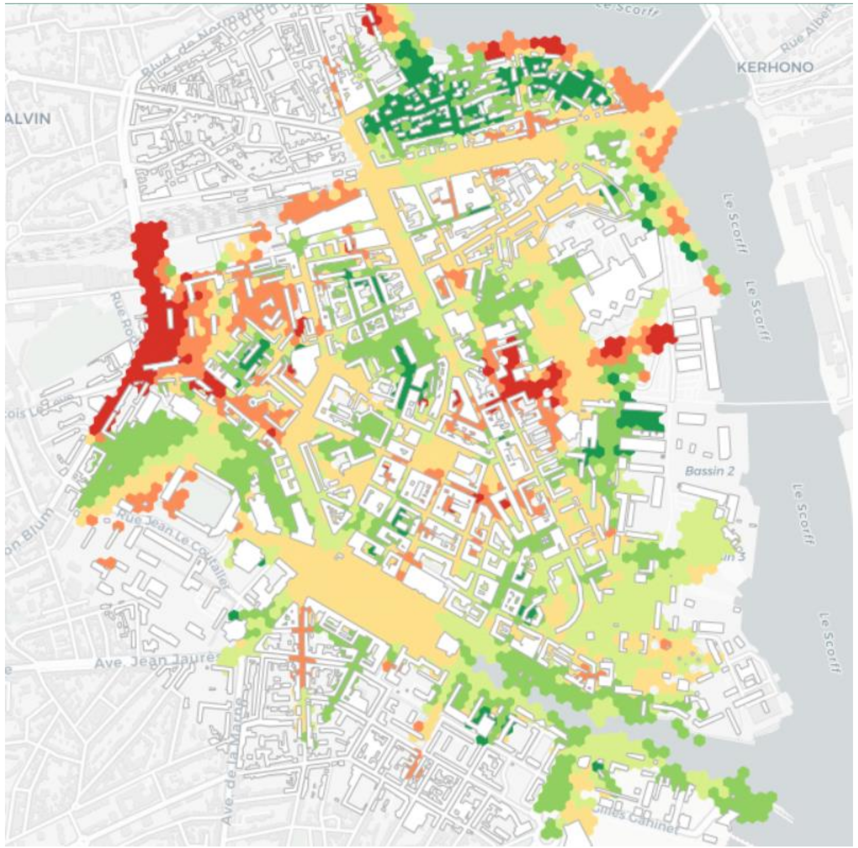

cense.noise-planet.org

Hong YJ.Y. (2017). Exploring spatial relationships among soundscape variables in urban areas: A spatial statistical modelling approach, Landscape and Urban Planning 157, 352–3
Kang, J., Aletta, F., Margaritis, E. Yang, M. (2018). A model for implementing soundscape maps in smart cities, Noise Mapping 5(1):46-59

Cartographies individualisées

Résidents peu sensibles

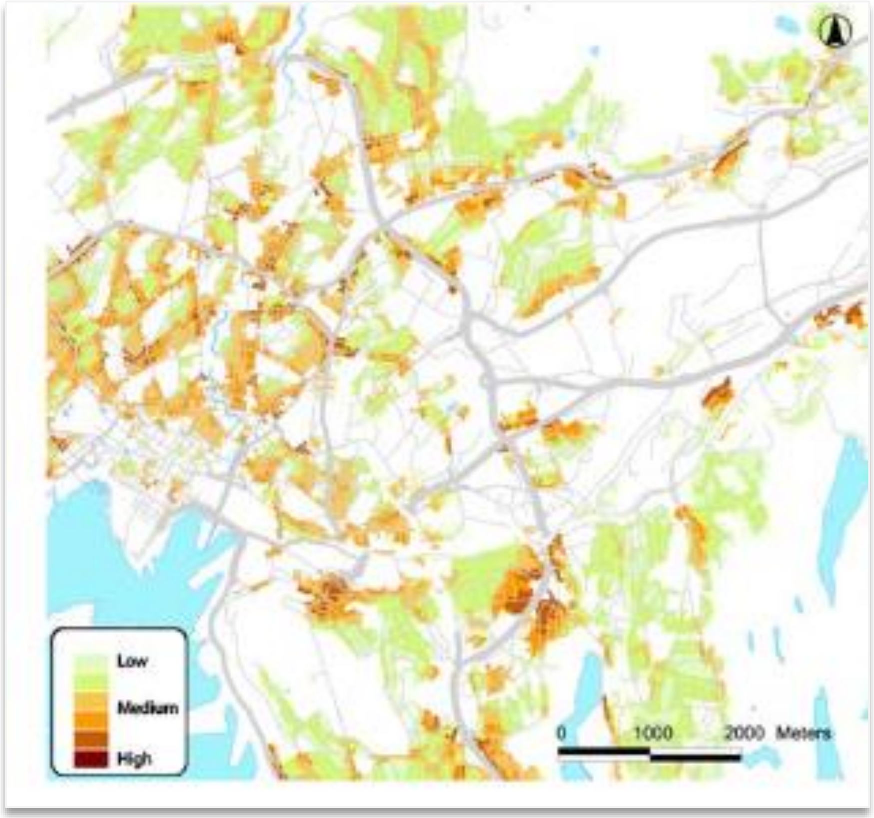

Résidents très sensibles

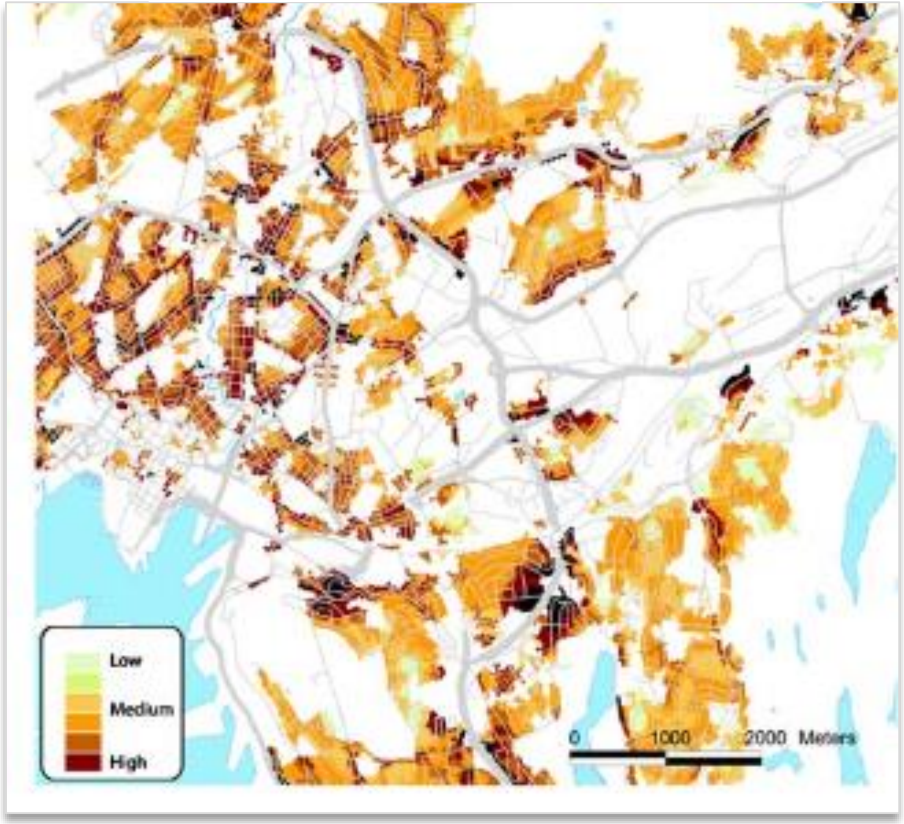

Klæboe, R., Engelien, E., Steinnes, M. (2006). Context sensitive noise impact mapping, Applied Acoustics, 67 (7), 620-642,

Reconnaissance des sources

Perceived sound level
$L_{50,1kHz}$ (or N_{50} or…)

Presence time of bird songs
$TFSD_{4kHz}$

Presence time of voices
$TFSD_{500Hz}$

Pleasantness

Rapport Final, projet ADEME GRAFIC, 2017

Reconnaissance des sources

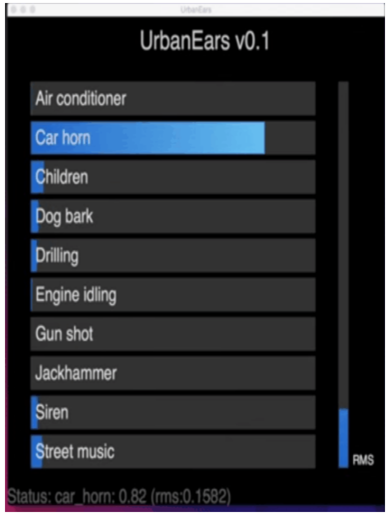

SONYC, 2017

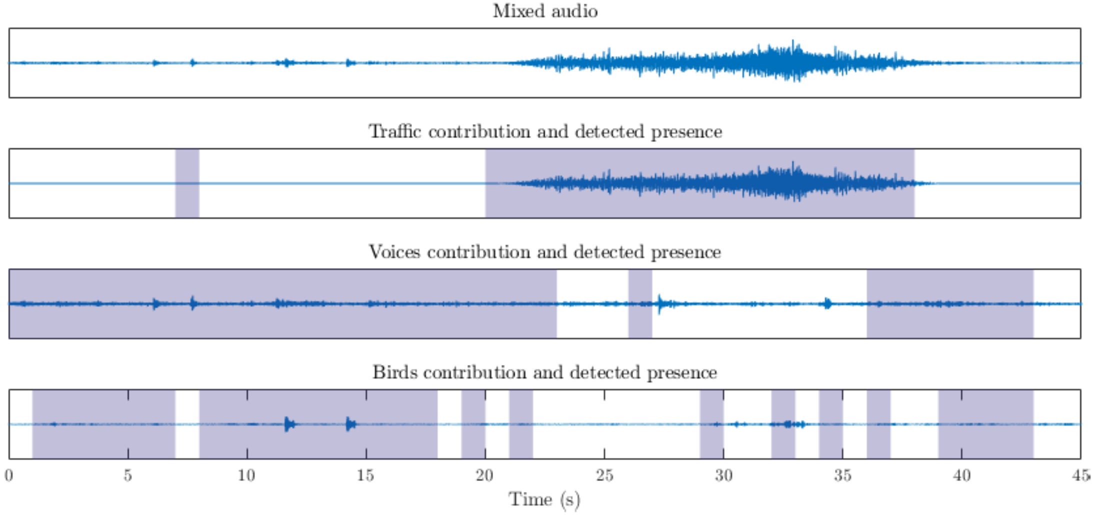

Analysis and interpretation of urban sound scenes using deep learning approache, F. Gontier, 2020

Quelques cartographies

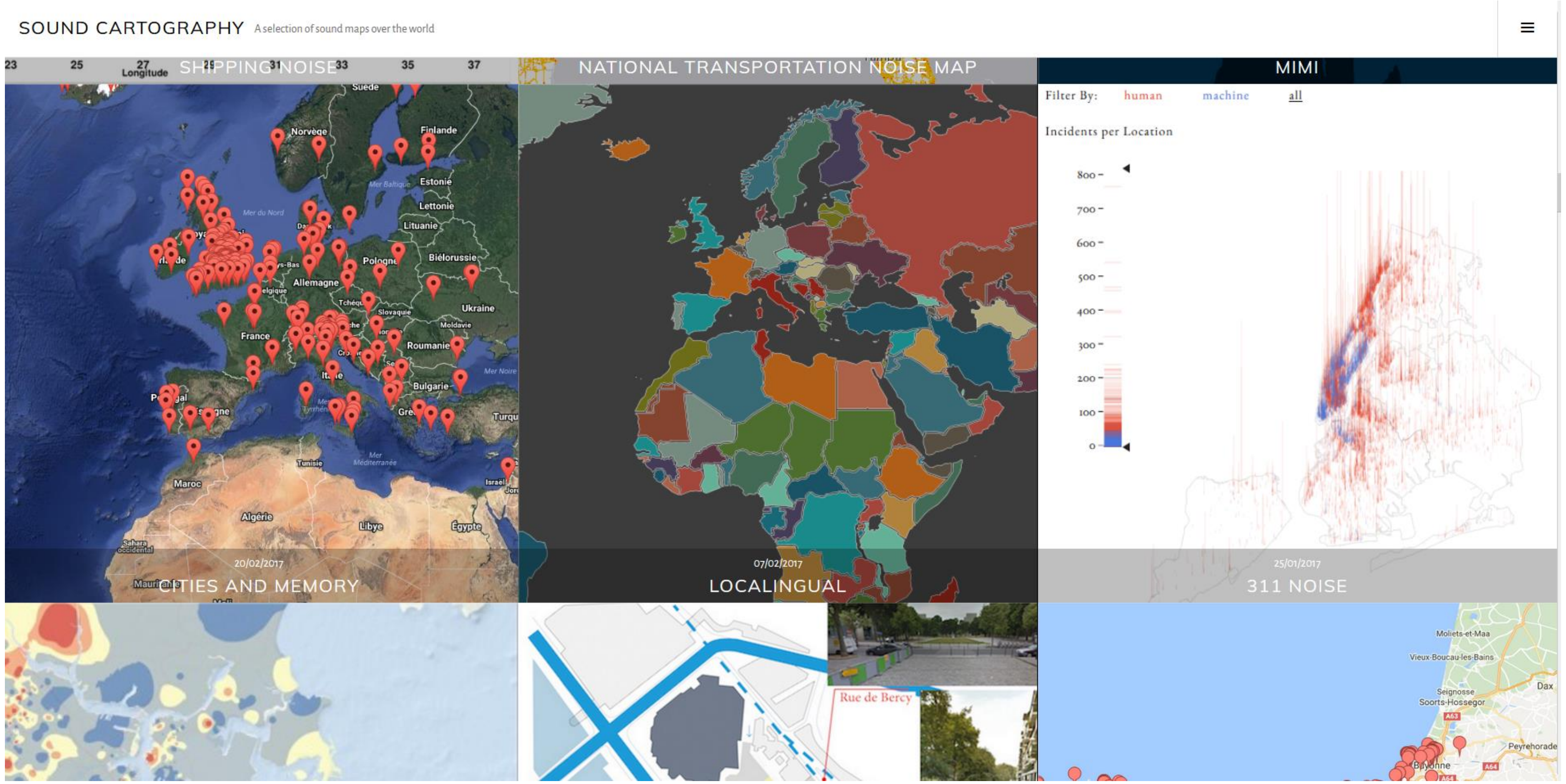

- Geolocalized recordings
- Measured sound
- Simulated sound
- Noise complaints
- Variety of sound sources
- Variety of representation
- From engineering to art

soundcartography.wordpress.com

Conclusion

Thank you !

Pierre AUMOND et les collègues du laboratoire !
Université Gustave Eiffel, CEREMA, UMRAE

Workshop SERENADE – 2022

www.umrae.fr
www.noise-planet.org
soundcartography.wordpress.com
pierre.aumond@univ-eiffel.fr

Segmentation

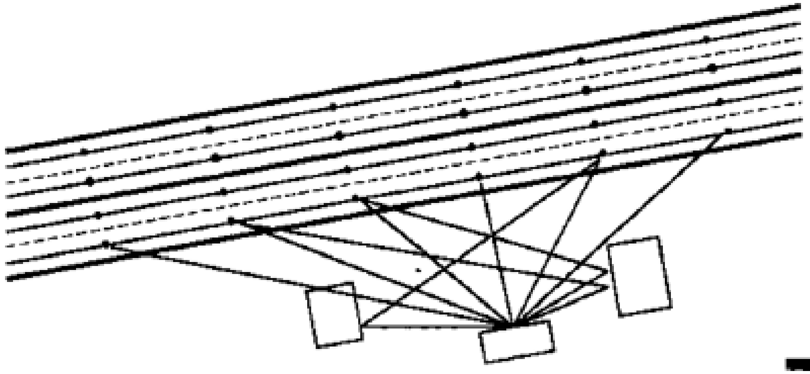

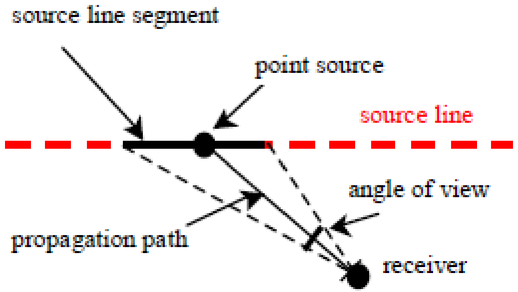

Figure I.4: *Source line, source line segment, propagation path and angle of view*

IV. Propagation

PathFinding

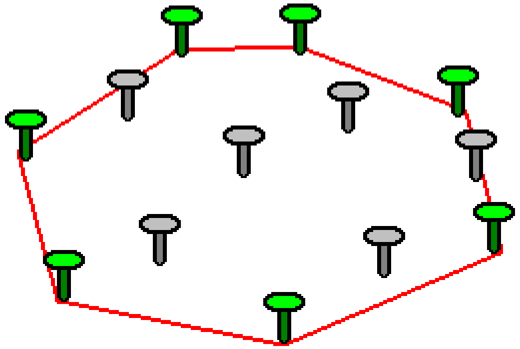

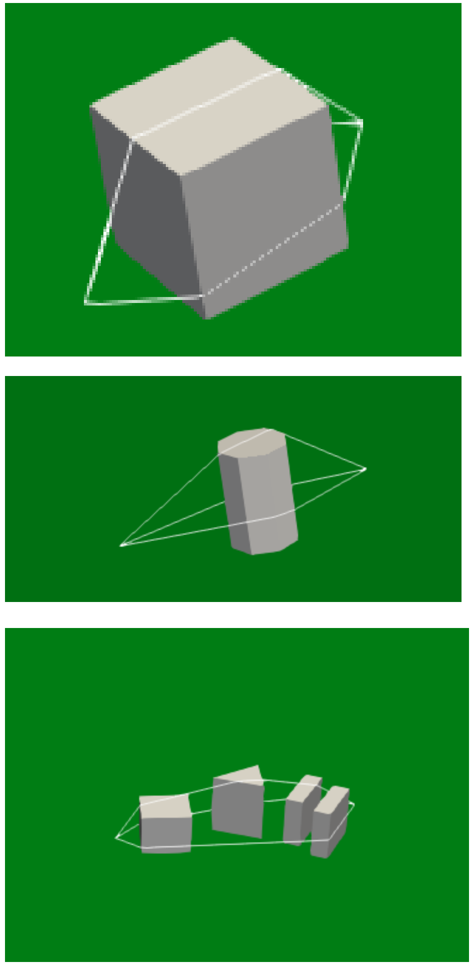

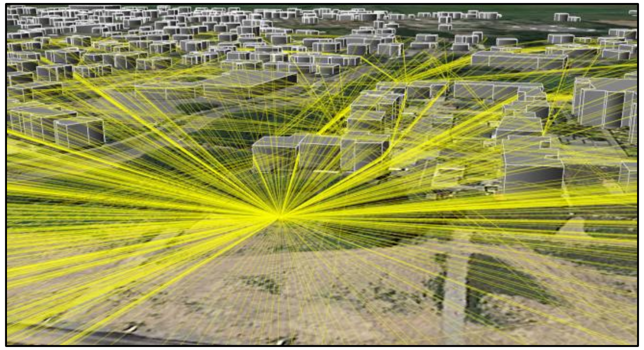

Attenuation

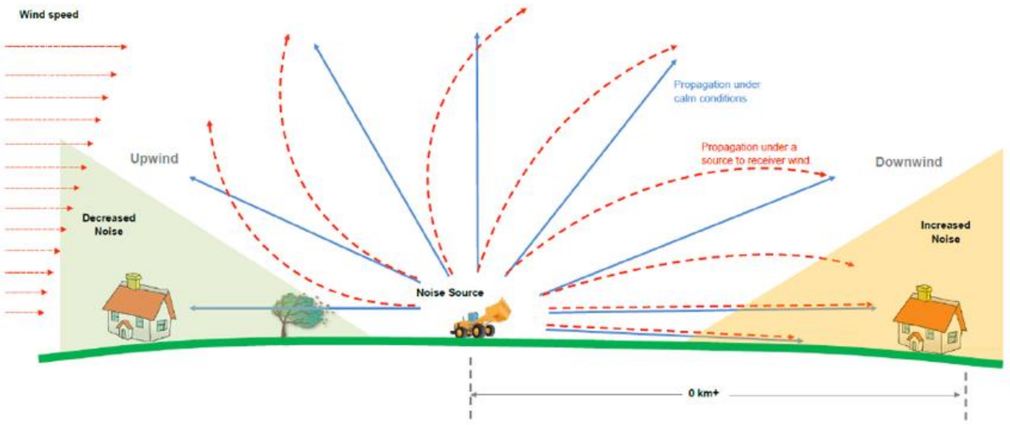

conditions homogènes

$L_H = L_W + A_H$ avec L_W le niveau de puissance de la source et

$A_H = A_{div} + A_{atm} + A_{sol} + A_{dif} + A_{meteo,H}$

conditions favorables

$L_F = L_W + A_F$ avec L_W le niveau de puissance de la source et

$A_F = A_{div} + A_{atm} + A_{sol} + A_{dif} + A_{meteo,F}$

Favourable conditions

$$L_{LT} = 10 \log \left[p \times 10^{L_F/10} + (1 - p) \times 10^{L_H/10} \right]$$

Θ = 0°　　Θ = 90°

Figure – Carte d'occurences nuit.

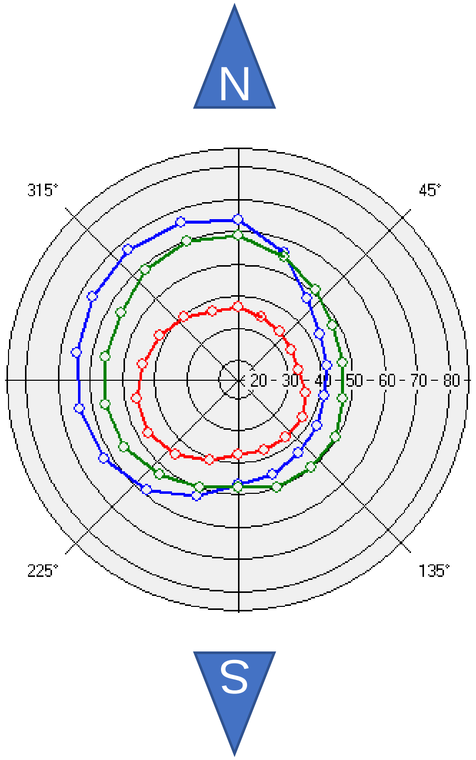

Attenuation

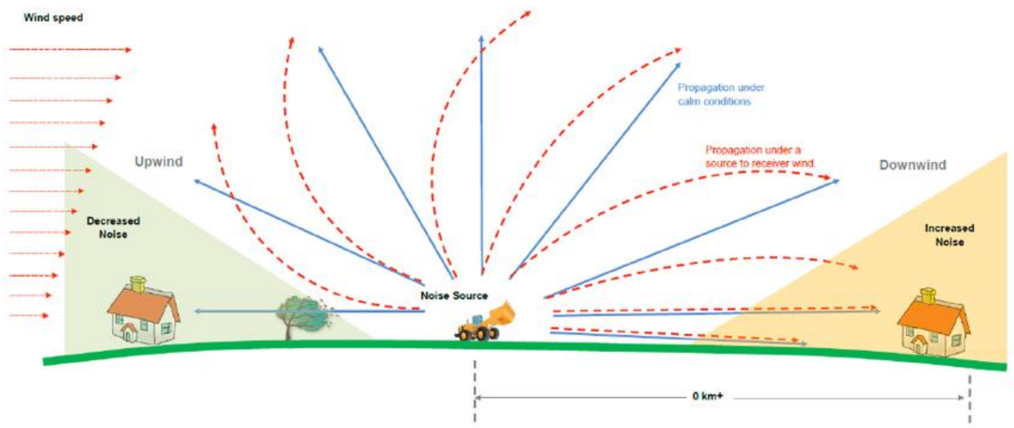

conditions homogènes

$L_H = L_W + A_H$ avec L_W le niveau de puissance de la source et
$A_H = A_{div} + A_{atm} + A_{sol} + A_{dif} + A_{meteo,H}$

conditions favorables

$L_F = L_W + A_F$ avec L_W le niveau de puissance de la source et
$A_F = A_{div} + A_{atm} + A_{sol} + A_{dif} + A_{meteo,F}$

Attenuation

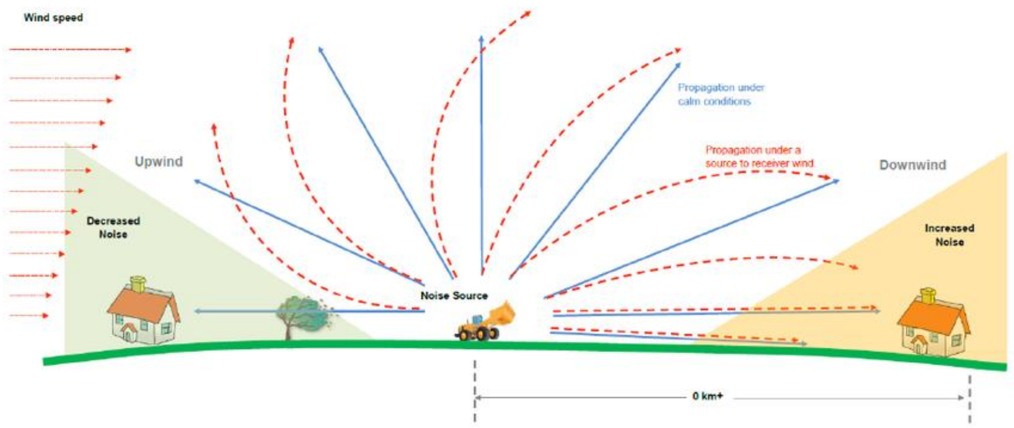

$$A_H = A_{div} + A_{atm} + A_{sol} + A_{dif} + A_{meteo,H}$$

Adiv

$$A_H = A_{div} + A_{atm} + A_{sol} + A_{dif} + A_{meteo,H}$$

$$A_{div} = 20 \times \lg(d) + 11$$

Aatm

$$A_H = A_{div} + A_{atm} + A_{sol} + A_{dif} + A_{meteo,H}$$

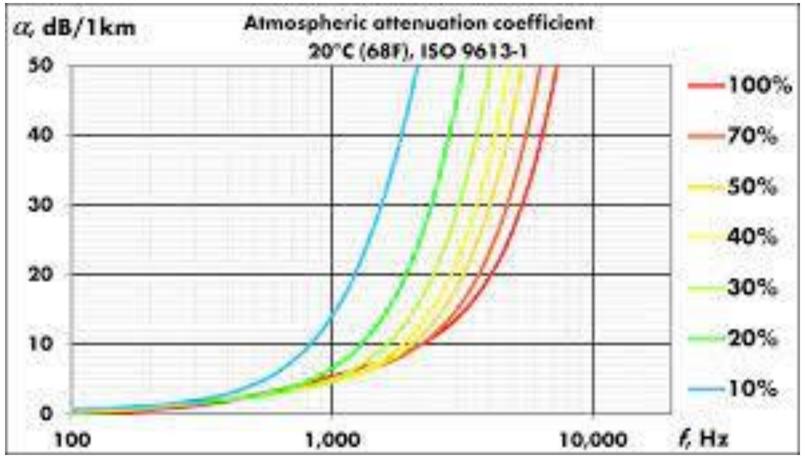

$$A_{atm} = \alpha_{atm} \cdot d / 1000$$

Aground

$$A_H = A_{div} + A_{atm} + A_{sol} + A_{dif} + A_{meteo,H}$$

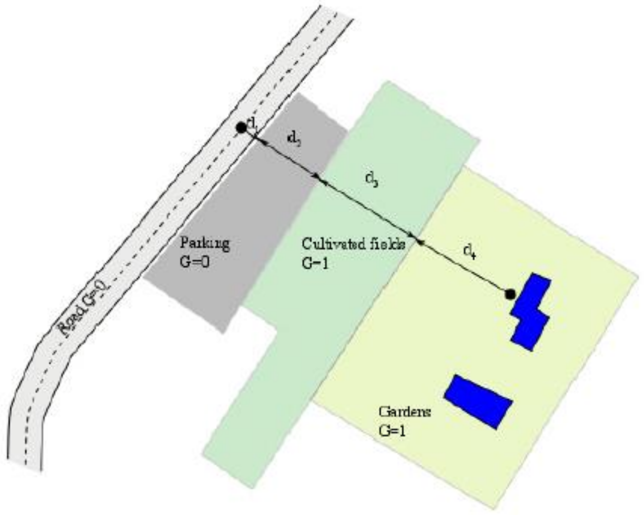

$$d = d_1 + d_2 + d_3 + d_4$$

$$G_{path} = \left(0 \cdot d_1 + 0 \cdot d_2 + 1 \cdot d_3 + 1 \cdot d_4\right) / d = \left(d_3 + d_4\right) / d$$

Figure VI.7: *Determination of the ground coefficient G_{path} over a propagation path*

Table VI.1: *G values for different types of ground*

Description	**Type**	**(kPa·s/m²)**	***G* value**
Very soft (snow or moss-like)	A	12.5	1
Soft forest floor (short, dense heather-like or thick moss)	B	31.5	1
Uncompacted, loose ground (turf, grass, loose soil)	C	80	1
Normal uncompacted ground (forest floors, pasture field)	D	200	1
Compacted field and gravel (compacted lawns, park area)	E	500	0.7
Compacted dense ground (gravel road, car park)	F	2000	0.3
Hard surfaces (most normal asphalt, concrete)	G	20 000	0
Very hard and dense surfaces (dense asphalt, concrete, water)	H	200 000	0

Aground

$$A_H = A_{div} + A_{atm} + A_{sol} + A_{dif} + A_{meteo,H}$$

Géométrie d'un calcul de l'atténuation due à la diffraction

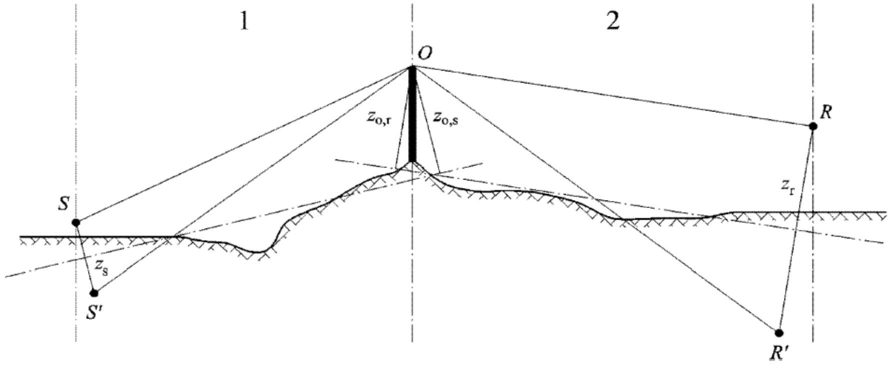

1: Côté source

2: Côté récepteur

$$A_{ground,H} = \max\left(-10\times\lg\left[4\frac{k^2}{d_p^2}\left(z_s^2-\sqrt{\frac{2C_f}{k}}z_s+\frac{C_f}{k}\right)\left(z_r^2-\sqrt{\frac{2C_f}{k}}z_r+\frac{C_f}{k}\right)\right], A_{ground,H,min}\right)$$

if $G_{path} = 0 : A_{ground,H} = -3$ dB

Adiff

$$A_H = A_{div} + A_{atm} + A_{sol} + A_{dif} + A_{meteo,H}$$

$$A_{dif} = \Delta_{dif\,(S,R)} + \Delta_{ground\,(S,O)} + \Delta_{ground\,(O_n\,,R)}$$

$$\Delta_{dif} = \begin{cases} 10C_h \cdot \lg\left(3 + \frac{40}{\lambda}C''\delta\right) & \text{if } \frac{40}{\lambda}C''\delta \geq -2 \\ 0 & \text{otherwise} \end{cases}$$

> 0 dB & < 25 dB

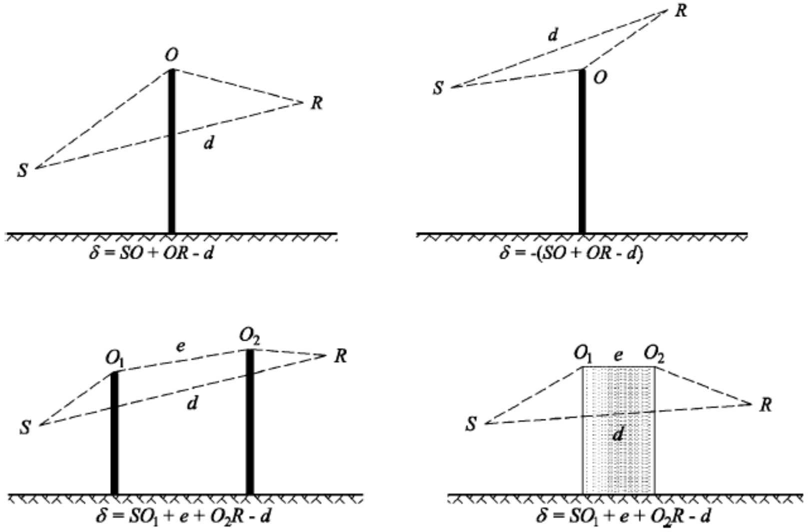

Figure VI.9: *Calculation of the path difference in homogeneous conditions. O, O_1 and O_2 are the diffraction points*

Note: For each configuration, the expression of δ is given.

Aref

$$A_H = A_{div} + A_{atm} + A_{sol} + A_{dif} + A_{meteo,H}$$

$$L_{W'} = L_W + 10 \times \lg\left(1 - \alpha_r\right)$$

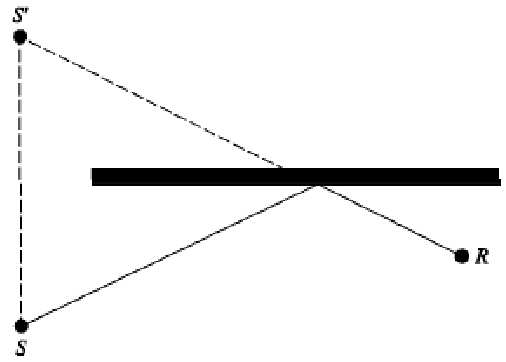

Figure VI.12: *Specular reflection on an obstacle dealt with by the image source method (S: source, S': image source, R: receiver)*

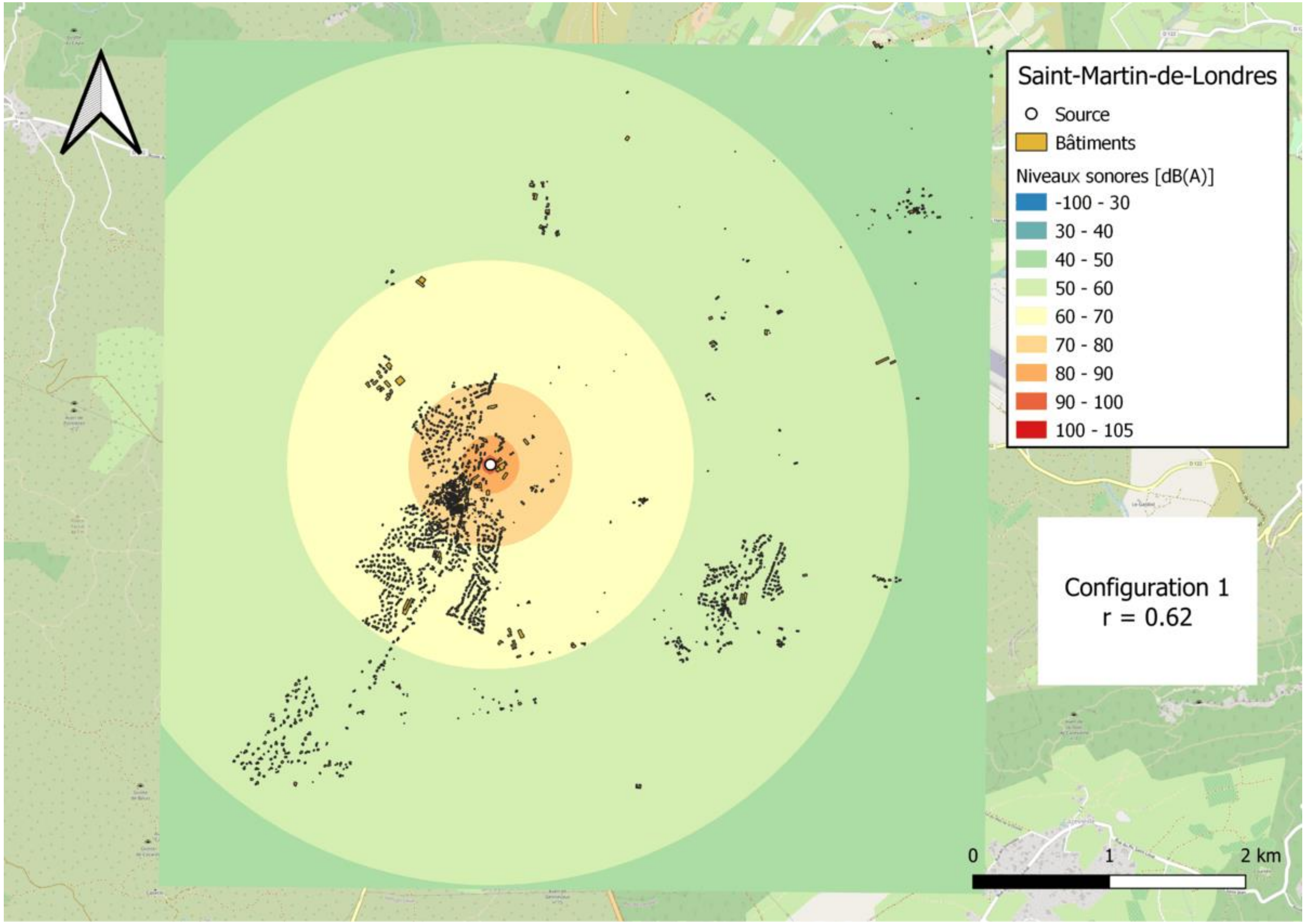
Saint-Martin-de-Londres
Source
Bâtiments
Niveaux sonores [dB(A)]
-100 - 30
30 - 40
40 - 50
50 - 60
60 - 70
70 - 80
80 - 90
90 - 100
100 - 105
Configuration 1
r = 0.62
0
1
2 km

IV. Limits

Given limits…

- Height receivers > 2m
- Distance < 800 m
- downward-refraction / homogeneous
- 63 Hz to 4 000 Hz – center band
- Breakdown of the infrastructures into point sources
- does not apply to propagation scenarios above a water body (lake, wide river, etc.).
- The effects of tunnel mouths are not dealt with by the method.
- This method considers obstacles to be equivalent to flat surfaces.

Known limits…

- Berm cannot be modelled
- Screen induced refraction
- Upward-refraction
- Constructive interferences